Title

The Rossiter equation: Improving the fractional vortex speed and defining an effective length to depth ratio for cavity flows

Journal

The Journal of the Acoustical Society of America, 155(2)

ISSN

0001-4966

Authors

Gabel, Matthew

Sarigul-Klijn, Nesrin

Publication Date

2024-02-01

DOI

10.1121/10.0024722

JASA ARTICLE

The Rossiter equation: Improving the fractional vortex speed and defining an effective length to depth ratio for cavity flows

Matthew Gabel and Nesrin Sarigul-Klijn[a)]
DynaaTECC Research Lab, Mechanical and Aerospace Engineering, University of California, Davis, Davis, California 95616-5294, USA

ABSTRACT:
This paper first reviews well known analytical techniques for predicting the Rossiter modes of a cavity in compressible flow. We combine existing methods to improve the performance in compressible flow. Second, we introduce a method based on an effective length to depth ratio of the cavity from experimental results for predicting frequencies across Mach numbers. Finally, the fractional vortex speed used in the Rossiter equation and its derivatives is calculated from high subsonic (M 0.55) to supersonic (M 2.3) for use in future cavity mode prediction.
 https://doi.org/10.1121/10.0024722

(Received 6 March 2023; revised 15 January 2024; accepted 17 January 2024; published online 5 February 2024)

[Editor: James F. Lynch] Pages: 952–961

NOMENCLATURE

L	Length of the cavity
U	Freestream velocity
U_c	Phase velocity
T	Static temperature
T_0	Stagnation temperature
D	Depth of the cavity
a	Phase velocity or speed of sound
λ_a	Acoustic wavelength
λ_v	Vortex wavelength
f_n	Resonant frequency corresponding to mode n
ω	Angular frequency
n	Mode
θ	Boundary layer thickness
V	Velocity
p	Pressure
γ	Ratio of specific heats, 1.4 for air
r	Thermal recovery factor, 0.9
R	Gas constant for air, equal to $287(J/kg \times K)$
M	Mach number
TE	Trailing edge
LE	Leading edge
κ	Fractional vortex convectional speed, 0.57 classically
ξ	Phase lag correction factor for edge effects
$+$	Used as subscript for downstream
$-$	Used as subscript for upstream
St	Strouhal number: $St = f_n L/U$, non-dimensional frequency

I. INTRODUCTION

Cavity flows are ubiquitous features in many aerospace systems and have been a topic of study since the early jet age.[1] Cavity flows are typically defined by their length to depth (L/D) ratio, called the cavity aspect ratio, and the Mach number or freestream velocity of the external flow. The fluid medium in question is most commonly air and will be treated as such in this work. Cavity flows display stable or unstable behavior, depending on the conditions. Stable cavity behavior is typically characterized by a stable vortex inside the cavity and is referred to as the shear mode.[2] The shear mode covers all cases detailed in this paper.

A Kelvin–Helmholtz-like instability occurs in the shear layer between the cavity and the freestream fluid, while upstream feedback occurs from acoustic waves.[3] The cavity is dominated by particular acoustic frequencies, commonly called the Rossiter modes, that arise from this feedback under certain flow conditions. Modes can be present simultaneously in the cavity,[4] and models predict multiple separate modes for this reason. However, one mode will typically dominate the cavity acoustic response and will affect experimental correlation.[5] Experiments have verified that the wavelengths of these acoustic modes correspond to the Strouhal number and the cavity geometry, as predicted by Rossiter.[6] The precise conditions these modes occur in will be detailed in Sec. II of the paper, but typically they occur in compressible flows for medium to high aspect ratio cavities.

Recent analysis of high-speed particle image velocimetry by Singh and Ukeiley[6] suggests that acoustic mode shapes present in the flow can exist independent of Mach number and depend mainly on the Strouhal number of the flow. Sun *et al.*[7] observed that the shear layer structures of these modes can grow in the cavity and lead to unwanted flow instabilities when they overflow and alter the modes' behavior in unexpected ways. Sun *et al.* also noticed increasing Mach number can have a stabilizing effect on these shear structures in supersonic flows but a destabilizing one in subsonic flows.[7]

The acoustic response of cavity flows can be poor for several reasons. The structural response to these oscillations can lead to fatigue or flutter failure,[4] and many of the first

[a)]Email: nsarigulklijn@ucdavis.edu

https://doi.org/10.1121/10.0024722

cavity investigations in aerospace science were in response to this. Noise is a large factor as well. Noise from the landing gear assemblies during takeoff and landing is typically a large contributor to the aircraft's total aerodynamic noise. The landing gear bay itself primarily contributes a portion of the lower frequency noise, which is of greater concern.[8] Drag can also be highly unfavorable from cavities.

Figure 1 shows a typical shear mode cavity flow with vocabulary and important quantities listed. Rossiter[9] initially classified the cavity behavior and empirically derived an equation for predicting the acoustic frequencies present in the cavity. Heller *et al.*[4] compared the acoustic response of cavities across Mach numbers and found they consistently produced the modes Rossiter predicted. Heller *et al.*[4] later modified Rossiter's equation by more accurately accounting for the acoustics inside the cavity. Dechant[10] has derived a similar novel equation using classical fluid mechanics and acoustics. Most recently, Casalino *et al.*[11] ran many computational simulations to classify the upstream flow present inside the cavity and improve the behavior of Rossiter's equation across all conditions. Despite the advent of many powerful computational methods, these analytical and empirical methods make relatively accurate predictions of the frequency for cavity flow pressure oscillations in the shear mode. Their main limitation is the equations are only valid for the particular flow conditions where the Rossiter modes occur.

In particular, the Rossiter equation suffers at higher Mach numbers outside of where it was semi-empirically derived. DeChant's and Casalino's methods are more robust. We will implement Heller's[4] and Casalino's[11] work into DeChant[10] to better handle compressibility effects. We will also add an additional term to modify the (L/D) ratio used in the DeChant[10] equation based on the vortical structures inside the cavity to help the method handle a wider range of conditions. We review the Rossiter[9] equation, the newer analytical method from DeChant,[10] Casalino,[11] the Block[12] equation, as well as our own modified forms of the DeChant[10] equation that account for compressibility and the vortex within the cavity. We attempt to classify the size of the vortex within mid-size cavities across Mach number using a collection of experimental results from other work. Additionally, we more precisely quantify the fractional vortex speed that Rossiter[9] defined in the Rossiter equation to make the method more accurate outside the range it was originally created for.

We compare these methods with three different test cases at Mach 0.55, 0.8, and 2.0 with aspect ratios of approximately 5 for all three cavities. The subsonic cases are from wind tunnel tests from Wagner *et al.*[13] where they studied how the width of cavities affects acoustic behavior. Wagner *et al.* noticed that the modal frequencies were consistent for different widths, but the sound pressure level could vary significantly. For the supersonic case, Zhuang *et al.*[14] looked at the use of microjets to divert supersonic flow away from a cavity to improve its behavior. They found use of the jets reduced cavity tones by up to 20 dB as well as significantly reduced flow unsteadiness inside of the cavity.

II. BACKGROUND AND METHODS

In 1964, Rossiter[9] developed what is probably the most well-known of the analytical equations to predict cavity flow oscillations. Rossiter noticed periodic density oscillations occur at the cavity mouth, which he attributed to

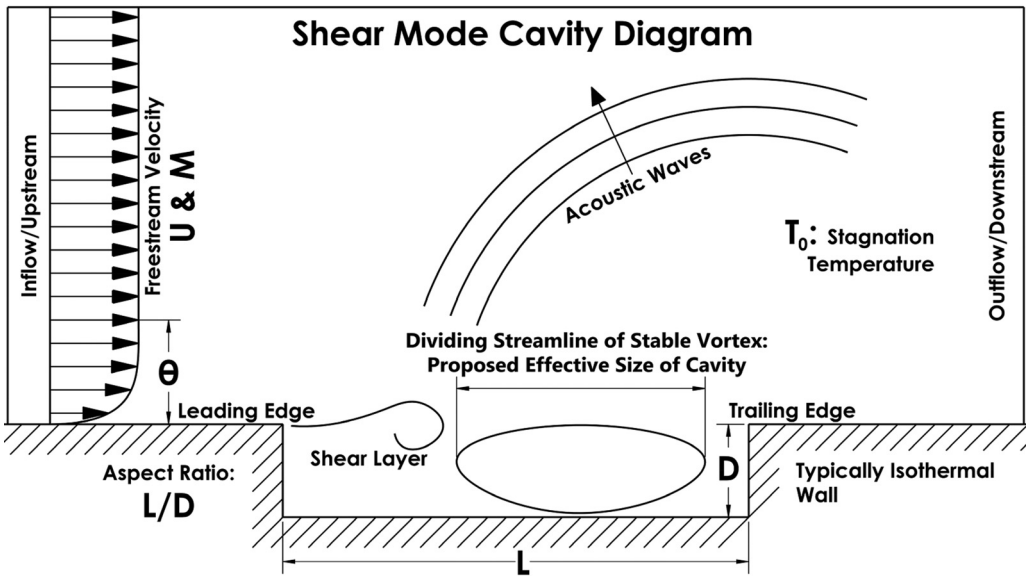

FIG. 1. Cavity flow diagram shown in the Rossiter mode. A feedback loop occurs between the shear layer moving downstream from the leading edge and acoustic waves traveling upstream from the trailing edge, generating stable vortices in the cavity. The cavity is primarily characterized by the freestream velocity, local speed of sound (in the Mach number), and the length to depth (L/D) ratio of the cavity. The cavity model is two dimensional; depth is neglected. θ is the boundary layer thickness; the boundary layer preceding the cavity also affects cavity behavior, but this is neglected in the analytical methods covered here.

vortices. Rossiter posited acoustic waves in the shear mode emanate from the trailing edge of the cavity. Rossiter developed an equation based on these observations and two main assumptions. The first assumption was the vortex shedding occurred at the same frequency as the acoustic waves. This made for a negligible recirculating velocity in the cavity, allowing the acoustic speed to only be the speed of sound upstream. Rossiter found this to be true if the L/D ratio was >1 for the cavity in transonic flows. Other work has proven this continues to be true for L/D ratios larger than 4 with higher Mach numbers, although accuracy is inferior to the originally specified domain.[15]

If the frequency of the vortex shedding and acoustics are the same, the ratio of the vortex speed to the vortex frequency must equal the ratio between the speed of sound and the wavelength of the sound propagated upstream. The vortex speed was taken as some fraction of the freestream velocity, as shown in Eq. (1):

$$f = \frac{\kappa U_+}{\lambda_v} = \frac{a_-}{\lambda_{a-}}. \tag{1}$$

The second condition Rossiter made was that the phase shift of the convected vortex coming from the leading edge plus the phase change of the acoustic wave going the opposite direction must be equal to the mode number multiplied by 2π and a correction factor, as shown in Eq. (2). The correction factor is experimentally determined for the phase lag due to the edge effects. Rossiter's results for the phase lag are tabulated in Table I. In Eq. (2),

$$2\pi L\left(\frac{1}{\lambda_v} + \frac{1}{\lambda_{a-}}\right) = 2\pi(n+\xi). \tag{2}$$

With substitutions, this leads to the following equation:

$$\frac{L}{\kappa U_+} + \frac{L}{a_-} = \frac{n-\xi}{f_n}. \tag{3}$$

The first term is the time it takes for the vortex to convect from the leading edge to the trailing edge. The second term is the time it takes the acoustic wave to travel in the opposite direction. Solving for the natural frequency and assuming the speed of sound is identical in both directions,

$$f_n = \frac{U_+}{L}\frac{n-\xi}{M_+ + \frac{1}{\kappa}}. \tag{4}$$

TABLE I. Phase lag correction factor for edge effects as a function of cavity aspect ratios (L/D ratios) of 4, 6, 8, and 10 (Rossiter).[a]

L/D ratio	ξ
4	0.25
6	0.38
8	0.54
10	0.58

[a]Reference 9.

This can be non-dimensionalized by dividing both sides by freestream velocity over cavity length, yielding the Strouhal number:

$$St_{\text{Rossiter}} = \frac{f_n L}{U_+} = \frac{n-\xi}{M_+ + \frac{1}{\kappa}}. \tag{5}$$

It is worth noting that this equation assumes the upstream speed of the acoustic wave is the same as the downstream speed because it uses the downstream speed of sound in the Mach number. This assumption is only truly accurate in low-speed, incompressible cases.

Heller *et al.*[4] found the accuracy of Eq. (5) is improved more generally by adding an isentropic relation for the stagnation sound speed Eq. (6).[16] This assumes the speed of sound in the upstream direction inside the cavity is equal to the stagnation speed of sound outside of the cavity. This assumption is valid as long as the cavity temperature is approximately equal to the freestream stagnation temperature, which Heller found true up to approximately Mach 3, where the error increases marginally:

$$\frac{a_-}{a_+} = \left(1 + r\left[\frac{\gamma-1}{2}\right]M_+^2\right)^{1/2}. \tag{6}$$

This acoustic relation is attached to the Mach number to yield the modified Rossiter equation:

$$f_n = \frac{U_+}{L}\frac{n-\xi}{M_+\frac{a_+}{a_-} + \frac{1}{\kappa}}. \tag{7}$$

This is non-dimensionalized to the Strouhal number, and the Mach number is simplified out:

$$St_{MR} = \frac{f_n L}{U_+} = \frac{N-\xi}{\frac{U_+}{a_-} + \frac{1}{\kappa}}. \tag{8}$$

DeChant[10] derived a Rossiter-like expression using an average of the acoustic and shear layer frequencies. The acoustic frequency was derived in the same manner as a Kelvin–Helmholtz instability, using the classical vortex sheet expressions to get the temporal behavior of the pressure field.[17] They then define two incompressible, inviscid parallel streams at an interface with a small velocity potential and solve the resulting Laplace equations using a normal mode approximation. DeChant[10] uses a Bernoulli assumption at the interface like the classical Kelvin–Helmholtz instability to calculate the phase velocity as

$$U_c = \frac{U_+}{1 + \coth\left(n\pi\frac{D}{L}\right)}. \tag{9}$$

DeChant[10] then solves the following acoustic problem for a rectangular cavity:

https://doi.org/10.1121/10.0024722

$$a_+^2\left(p'_{yy}+p'_{xx}\right)=p'_{tt}. \tag{10}$$

This expression is solved with the standard boundary conditions for a cavity and a separation of variables approach. The approach most importantly yields an expression for the acoustic temporal frequency, as shown below in Eq. (11). This also assumes the upstream speed of sound is the same as the downstream speed, which is only entirely true for a purely incompressible flow. To show this assumption, the speed of sound is displayed with the downstream subscript even though it is in the upstream direction:

$$\omega_a=a_+\pi\frac{n}{L}. \tag{11}$$

Using Eq. (9) for the phase speed, the shear layer frequency is

$$\omega_s=\frac{n\pi}{L}U_c. \tag{12}$$

DeChant[10] now argues that upstream and downstream velocities within the cavity are simply these angular frequencies multiplied by the cavity length. If the characteristic velocity of the cavity is the average velocity of an upstream and downstream cycle, then the characteristic velocity is simply

$$V_{\text{char}}=\frac{2L}{\frac{1}{\omega_a}+\frac{1}{\omega_s}}=\frac{2L}{\frac{L}{V_{up}}+\frac{L}{V_{\text{down}}}}=\frac{2}{V_-^{-1}+V_+^{-1}}. \tag{13}$$

The average frequency will thus follow in the same way: Rearranged to

$$\omega_{\text{ave}}=\frac{2}{\frac{1}{\omega_a}+\frac{1}{\omega_s}}=\frac{\omega_a\omega_s}{\frac{1}{2}(\omega_a+\omega_s)}, \tag{14}$$

$$2\pi f=\frac{2\pi n}{\frac{L}{a_+}+\frac{L}{U_c}}. \tag{15}$$

The known expressions for angular frequency are plugged in, the frequency is converted from angular to ordinary, and the equation is non-dimensionalized to the Strouhal number:

$$St_{\text{DeChant}}=\frac{n}{M_+ +\frac{U_+}{U_c}}. \tag{16}$$

This model is very Rossiter like in behavior but is more rigorously derived from classical fluid mechanics and the known flow physics. When the phase velocity relation is incorporated, Eq. (16) is expressed as

$$St_{\text{DeChant}}=\frac{f_{\text{DeChant}}L}{U_+}=\frac{n}{M_+ +\left\{1+\coth\left[n\pi\left(\frac{L}{D}\right)^{-1}\right]\right\}}. \tag{17}$$

This method works well in the subsonic regime of the Rossiter modes and presents an equation that is much more robustly derived from formal fluid mechanics than previous empirical relations.

We would like to improve this method in two ways. The first is to include compressibility effects on the upstream acoustics discussed previously to help improve accuracy at higher Mach numbers. We add a new term for the L/D ratio input as the second modification to this method. DeChant[10] assumed the upstream speed of sound was identical to the downstream in their derivation, just like Rossiter.[9] This modification is completed in the same manner as the Rossiter modification, by multiplying the downstream Mach number by the ratio of the downstream to upstream speed of sound found from the isentropic relation given before in Eq. (6):

$$\frac{fL}{U_+}=\frac{n}{M_+\frac{a_+}{a_-}+\left\{1+\coth\left[n\pi\left(\frac{L}{D}\right)^{-1}\right]\right\}}. \tag{18}$$

This simplifies to the following relation if we incorporate the upstream speed of sound:

$$St=\frac{fL}{U_+}=\frac{n}{\frac{U_+}{a_-}+\left\{1+\coth\left[n\pi\left(\frac{L}{D}\right)^{-1}\right]\right\}}. \tag{19}$$

The feedback mechanism discussed previously in Eqs. (9)–(15) was essentially a relation between a vortex sheet generated by a shear layer traveling downstream and acoustic waves traveling upstream. This mechanism was assumed to persist from the leading to the trailing edge of the cavity and generate the acoustic modes we are interested in.

While the Rossiter modes are present, a stable vortex also persists inside the cavity in a shear mode. This vortex arises from the same mechanisms that produce our Rossiter frequencies. The stable vortex present inside the cavity only fills a section of the length in many cavities, especially at higher Mach numbers. We hypothesize that if the vortex does not fill the entire cavity, it suggests that the feedback mechanism for the acoustic modes is not based on the full L/D ratio either. This can be corrected for by multiplying the length by the vortex size to cavity length ratio. This corrected length will be referred to as the effective length of the cavity. This method will be referred to as the current method from now on and is shown below:

$$\begin{aligned}St_{\text{current}}&=\frac{n}{M_+\frac{a_+}{a_-}+\left\{1+\coth\left[n\pi\left(\frac{L}{D}*\frac{L_{eff}}{L}\right)^{-1}\right]\right\}}\\&=\frac{n}{\frac{U_+}{a_-}+\left\{1+\coth\left[n\pi\left(\frac{L_{\text{eff}}}{D}\right)^{-1}\right]\right\}}.\end{aligned} \tag{20}$$

In the case of the test cases used in this paper, the vortex length to cavity length ratio can be most easily found by

looking at the mean streamline velocity contours presented from wind tunnel experiments.[13,14] The size of the vortex is estimated by using the color map or by the largest streamline that closes around the vortex.

Recently, Casalino *et al.*[11] revised the Rossiter formula in two ways. A second order polynomial approximation was introduced for the phase lag correction factor, as shown in Eq. (21):

$$\xi_{2\text{nd}} = -0.0056\left(\frac{L}{D}\right)^2 + 0.1363\left(\frac{L}{D}\right) - 0.2125. \tag{21}$$

The second major modification was the implementation and characterization of the recirculation velocity inside the cavity. The soundwaves traveling upstream in the cavity are carried by upstream velocity gradients from the persistent cavity vortices. Casalino *et al.*[11] created an expression for an average recirculation velocity upstream using data aggregation from computational simulations with a range of different cavity conditions. The velocity in the equation below is non-dimensional in terms of the freestream velocity and is a polynomial fit of their results:

$$\tilde{V}_{\text{recirc}}\left(\frac{L}{D}, M_+\right) = \mu_0 + \mu_1\frac{L}{D} + \mu_2 M_+ + \mu_3\left(\frac{L}{D}\right)^2 + \mu_4 M_+^2 + \mu_5 M_+\frac{L}{D}. \tag{22}$$

Casalino *et al.*[11] characterize this reversed flow velocity along two different lines in the cavity 5 mm and 10 mm above the cavity floor. There was no criterion for an optimal acoustic path, which limited the authors to a spatial average approach. Both average lines for velocity were firmly in the reverse flow region and outside the boundary layer inside the simulated cavities. The polynomial coefficients along the average lines are classified in Table II below. In this work, we exclusively use the coefficients from the 5 mm line because the error is less.

The reversed flow velocity was converted into a local Mach number for implementation into the Rossiter equation, as shown in Eq. (23) below:

$$M_{\text{recirc}}\left(\frac{L}{D}, M_+\right) = \frac{M_+}{\left(1 + \left[\frac{\gamma-1}{2}\right]M_+^2\right)^{\frac{1}{2}}}\tilde{V}_{\text{circ}}\left(\frac{L}{D}, M_+\right). \tag{23}$$

This along with the modified phase lag correction factor was implemented into the modified Rossiter equation, Eq. (8), to yield the following equation:

$$St_{\text{Casalino}} = \frac{f_n L}{U_+} = \frac{(n - \xi_{2\text{nd}})(1 + M_{\text{recirc}})}{\frac{U_+}{a_-} + \frac{1 + \text{M}_{\text{recirc}}}{\kappa}}. \tag{24}$$

It is worth nothing that Casalino *et al.*[11] do not implement the thermal recovery factor into their isentropic relationship equation, Eq. (6), to calculate the local speed of sound inside the cavity in Eqs. (23) and (24). Withholding the thermal recovery factor slightly increases the error compared to the experiment.

A second novel method modification is created by implementing the recirculation velocity expression Eq. (22) from Casalino *et al.*[11] into the modified DeChant equation, Eq. (19). This provides a full accounting of upstream contributions to the cavity's characteristic velocity in Eq. (13). This method will be referred to as upstream DeChant for the remainder of this report:

$$St_{-\text{DeChant}} = \frac{fL}{U_+} = \frac{n}{\frac{U_+}{a_- + U_+\tilde{V}_{\text{recirc}}} + \left\{1 + \coth\left[n\pi\left(\frac{L}{D}\right)^{-1}\right]\right\}}. \tag{25}$$

Another method we compare to is the work of Block *et al.*[12] from NASA Langley. Block *et al.* most noticeably included the L/D ratio explicitly in an equation they derived by comparing directly to experimental results. Block *et al.* looked at how the lengthwise vortical-acoustic modes interacted with depthwise standing-wave modes inside the cavity. The following expression was found based on those relations:

$$f_{\text{Block}} = \frac{n}{\frac{1}{\kappa} + M\left(1 + \frac{0.513}{\frac{L}{D}}\right)}. \tag{26}$$

Block was specifically designed for L/D ratios greater than 1 and for the transonic regime, but DeChant[10] found good agreement for supersonic cases. This method is not particularly accurate but was included for completeness because it has been used for comparison by other works.

The papers used as test cases typically provide stagnation temperature and Mach number from their experimental setup. Those quantities are used in the following isentropic flow equations, Eqs. (27) and (28), to find the static temperature and freestream speed of sound:

TABLE II. Polynomial expansion coefficients in Eq. (22) from Casalino *et al.*[a]

Line	μ_0	μ_1	μ_2	μ_3	μ_4	μ_5	Error
5 mm	0.286 526	−0.008 972	−0.108 192	0.0009	0.105 768	−0.009 661	9.8×10^{-4}
10 mm	0.274 566	−0.009 870	−0.092 915	0.0014	0.105 714	−0.013 085	1.1×10^{-3}

[a]Reference 11.

https://doi.org/10.1121/10.0024722

$$\frac{T_0}{T} = 1 + \frac{\gamma - 1}{2} M^2, \tag{27}$$

$$a = \sqrt{\gamma RT}. \tag{28}$$

III. RESULTS AND DISCUSSION

Specific parameters were adjusted in the equations to visualize how the methods compare and how the solutions differ for separate conditions. The Mach number of the flow was adjusted to visualize the effects on the Rossiter equation, the alternative methods, and our current approach. Figure 2 shows the frequency response of the first mode in a cavity with varying L/D ratios for 3 different Mach numbers corresponding to the test cases examined later in this report.

It is worth noting that the effective length of the cavity is assumed constant across the L/D ratio here so the methods can be compared, but the effective length is probably at least somewhat dependent on L/D ratio, especially outside of the range that Rossiter specifies. "Modified" refers to the implementation of the isentropic speed of sound ratio.

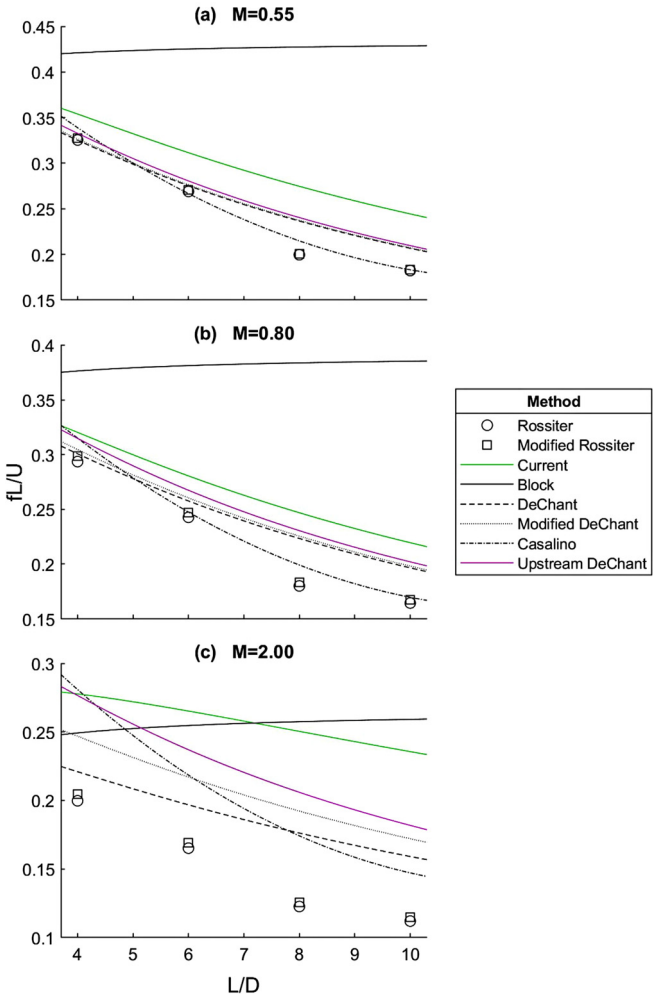

FIG. 2. (Color online) Frequency variation over length to depth (L/D) ratios for different Mach numbers under test case conditions. The Rossiter equations in Eqs. (5) and (8) are represented at discreet points corresponding to the phase lag correction factor values taken from Table I. The largest variation between methods generally occurs at higher Mach numbers and L/D ratios.

The difference between the Rossiter equation in Eq. (5) and modified Rossiter equation in Eq. (8) is most noticeable at higher Mach numbers, where there is a larger discrepancy between the speed of sound upstream in the cavity and downstream in the freestream. The Casalino equation [Eq. (24)] agrees most closely with other Rossiter derived methods for lower Mach numbers but diverges significantly as the Mach number increases the internal recirculation velocity The modified equations in Eqs. (8), (19), (20), (24), and (25) yield higher frequencies because the speed of sound in the upstream direction in the cavity is higher than the freestream, resulting in a shorter period and higher resulting frequency. At higher Mach numbers, the smaller vortex size in the cavity increasingly comes into play, resulting in peak frequency for our current method, Eq. (20), the Casalino equation, Eq. (24), and the upstream DeChant equation, Eq. (25), at a larger discrepancy from the other methods. The results diverge more between the Dechant equation, Eq. (17), and the current method, Eq. (20), at higher L/D ratios. The upstream DeChant [Eq. (25)] and Casalino [Eq. (24)] equations both diverge more from their respective base methods at lower L/D ratios. Dechant's model in Eq. (17) shows good agreement with the Rossiter methods in Eqs. (5) and (8) for all modes and across velocity regimes. Higher L/D ratios also cause a larger difference between the Dechant derived methods in Eqs. (17), (19), (20), and (25) and the Rossiter derived methods in Eqs. (5), (8), and (24). Of the existing models, the Block method, Eq. (26), has the poorest agreement with other methods, as DeChant[10] also noted.

A. Validation of method and comparison with test cases

Three experimental cases were chosen for method comparison and validation from papers that included experimental streamline or velocity contours so the vortex size could be accurately measured. The two subsonic cases were from a paper by Wagner *et al.*[13] that discussed aspect ratio effects on cavity frequency response. The precise size of the vortex had to be inferred based on the curvature of the streamlines because their results did not show the entire cavity due to limitations of their experimental apparatus. The cavity length to width ratio and the L/D ratio from Wagner *et al.*[13] were 5.0 for both cases.

The supersonic case came from a paper by Zhuang *et al.*[14] examining the flow behavior of supersonic cavities and their control with leading edge microjets to minimize unsteadiness. A velocity contour plot was used for vortex size for the supersonic case.

The vortex size was treated as being represented by the mean velocity contours inside the cavity corresponding to at least 10% of the freestream velocity magnitude. The Rossiter mode frequencies were measured for all three cases from sound pressure level plots included in the reports. CAD software was used to precisely measure the frequency values and vortex sizes from the papers. Zhuang *et al.*[14] report the

TABLE III. Mach 2 test case method comparison.[a]

	Strouhal no. $\frac{fL}{U}$ (% error from experiment)						
Mode	Experiment	Rossiter	Modified Rossiter	DeChant	Current	Casalino	Upstream DeChant
1	0.2624	0.1796 (31.6)	0.2056 (21.6)	0.2065 (21.3)	0.2657 (1.2)	0.2424 (7.6)	0.2621 (0.1)
2	0.5628	0.4459 (20.8)	0.5105 (9.3)	0.4770 (15.2)	0.5637 (0.1)	0.6108 (8.5)	0.6316 (12.2)
3	0.8911	0.7123 (20.1)	0.8155 (8.5)	0.7401 (16.9)	0.8505 (4.6)	0.9793 (9.9)	0.9910 (11.2)
4	1.2307	0.9787 (20.5)	1.1204 (9.0)	0.9961 (19.1)	1.1347 (7.8)	1.3477 (9.5)	1.3381 (8.7)

[a]$T_0 = 336\,K$, $L/D = 5.17$, and $L_{EFF}/L \approx 0.54$.

first mode as approximately 1.46 kHz, while we treat the first mode as the earlier peak at approximately 1.18 kHz, which is in line with theory. The cavity length to width ratio was 5.92 and the L/D ratio was 5.17 for their test case. Stagnation temperature was used with the Mach number to find the static temperature [Eq. (27)]. From there, the speed of sound [Eq. (28)] and freestream velocity of the flow could be derived. The results are tabulated in Table III, Table IV, and Table V for three test cases. Percent error is displayed in parentheses.

The Rossiter methods struggle at higher Mach numbers. Incorporating compressibility effects improves Rossiter's accuracy marginally in supersonic flow, but the accuracy is still inferior to subsonic conditions. DeChant's method is comparable to Rossiter in subsonic flow, and both are quite accurate in this regime overall. DeChant's method seems more robust for supersonic flow than Rossiter's, especially for the first mode. This is to be expected because DeChant's method was derived rigorously from flow physics, whereas Rossiter's method comes from empirically derived trends. At Mach 0.55, the differences between the Rossiter and modified Rossiter equations are also very minor, as one would expect nearing the edge of compressibility. Rossiter's equations tend to be more accurate for predicting higher modes. Casalino's method overcomes Rossiter's shortcomings at higher Mach numbers and is overall a general improvement in accuracy, but it struggles more for the first mode. The lowest Mach number case is the strongest for Casalino. Upstream DeChant performs comparably to marginally better versus Casalino for all 3 cases. The current method is quite accurate for all cases, especially for the 1st mode, compared to the others. The main complication is that you would need to measure the vortex size for a given cavity before you could make accurate frequency calculations.

B. Vortex size predictions

Ideally, we could catalogue the vortex size for a range of different conditions and define an analytical equation that could be used to quickly estimate the vortex size for a given cavity. Very few papers seem to include streamline visualization for their cavity flows, which makes cataloging vortex size in the cavity difficult. We attempted to work around this by collecting Rossiter mode data from several papers and then used numerical optimization to find what the vortex length should be to minimize the error across the first 4 modes. The code relies on optimization instead of least squares, so additional variables could be added as needed for establishing a trend in future work. The code worked by inputting the full possible range of different length ratios [0, 1] and then finding the value that minimized the cumulative error of the first 4 modes. We decided to prioritize the accuracy of lower modes in the optimization. The weighting for the four modes was [1, 0.9, 0.8, 0.7], respectively, but using an equal weighting did not substantially alter results. The numerically optimized values for an effective length ratio found for the three previous test cases are relatively in line with our measured vortex sizes (Table VI).

We attempted to keep the L/D ratio of the cavity to be near 5 for the data because the relationship between vortex length and cavity L/D ratio has not been established yet. The cavity ratios can be seen in the Fig. 3 legends. Figure 3 shows the weighted cumulative mode error and the vortex length ratios across Mach numbers. Weighted cumulative mode error refers to the weighted sum of the error across modes for each case.

The results of this optimization exercise are not entirely satisfactory. There is too much variation to establish an adequate trendline or least squares regression. Kaufman *et al.*[18]

TABLE IV. Mach 0.8 test case method comparison.[a]

	Strouhal no. $\frac{fL}{U}$ (% error from experiment)						
Mode	Experiment	Rossiter	Modified Rossiter	DeChant	Current	Casalino	Upstream DeChant
1	0.3199	0.2682 (16.2)	0.2727 (14.7)	0.2781 (13.0)	0.2999 (6.3)	0.2789 (12.8)	0.2898 (9.4)
2	0.7019	0.6596 (6.0)	0.6708 (4.4)	0.6720 (4.3)	0.6985 (0.5)	0.6945 (1.1)	0.7064 (0.6)
3	1.0765	1.0511 (2.4)	1.0689 (0.7)	1.0537 (2.1)	1.0790 (0.2)	1.1101 (3.1	1.1102 (3.1)
4	1.4474	1.4426 (0.3)	1.4670 (1.4)	1.4219 (1.8)	1.4479 (0.0)	1.5257 (5.4)	1.4991 (3.6)

[a]$T_0 = 321\,K$, $L/D = 5.00$, and $L_{EFF}/L \approx 0.84$.

https://doi.org/10.1121/10.0024722

TABLE V. Mach 0.55 test case method comparison.[a]

	Strouhal no. $\frac{fL}{U}$ (% error from experiment)						
Mode	Experiment	Rossiter	Modified Rossiter	DeChant	Current	Casalino	Upstream DeChant
1	0.3260	0.2973 (8.8)	0.2991 (8.2)	0.2989 (8.3)	0.3323 (2.0)	0.3003 (7.9)	0.3051 (6.4)
2	0.7561	0.7312 (3.3)	0.7358 (2.7)	0.7336 (3.0)	0.7658 (1.3)	0.7478 (1.1)	0.7525 (0.5)
3	1.1991	1.1652 (2.8)	1.1725 (2.2)	1.1551 (3.7)	1.1766 (1.9)	1.1953 (0.3)	1.1864 (1.1)
4	1.6348	1.5991 (2.2)	1.6092 (1.6)	1.5605 (4.5)	1.5759 (3.6)	1.6428 (0.5)	1.6034 (1.9)

[a]$T_0 = 321\,K$, $L/D = 5.00$, and $L_{EFF}/L \approx 0.76$.

and Bauer *et al.*[19] were older sources for several of the cases used in the optimization, and the accuracy of their results is inferior to the modern results we had used previously for our test cases. Kaufman *et al.*[18] used hand drawn graphs to show their frequency results, and the conditions in their wind tunnel were not reported precisely. The effective length ratio term in Eq. (20) is sensitive to error meaning the experimental results used in the optimization must be accurate to establish a proper trend. The Mach 1.5 point was taken from a paper by Casper *et al.*[15] for a cavity with an aspect ratio of 7 and similar conditions to the other tests. Future work could be done in the wind tunnel or with numerical simulation to gather results for vortex size. As a next step, we could run computational simulations and pull from other computational papers to further establish a trend for the effective length of the cavity. As it stands, for us there is strong indication of correlation because the optimization code produced similar results to what we measured from the contours.

We expected there to be different trends for the subsonic and supersonic regimes, and there does seems to be a difference in trends between the subsonic and supersonic results. The general trend of the data is consistent with the results of Sun *et al.*[7] Sun *et al.* observed the vortical structures growing outside the cavity near Mach 1 but gradually reduced again above Mach 1.2. This instability is consistent with the highest cumulative mode error occurring in the transonic regime. The break in the effective cavity size method occurring where vortical structures grow past the length of the cavity is a compelling explanation for the error seen.

C. Fractional vortex speed predictions

The same optimization code was rewritten to optimize the fractional vortex speed used in the Rossiter and Casalino equations in Eqs. (5), (8), and (24). Kaufman *et al.*[18] had previously experimentally derived the fractional vortex speed after Rossiter's work, but the reported values were not for a comprehensive range of Mach numbers. Our numerical optimization for the fractional vortex speed uses the same weighting for the modes as the vortex length code [1, 0.9, 0.8, 0.7]. The cumulative errors of the results for the

TABLE VI. Measured versus optimized fractional vortex size for the current method.

$\frac{L_{EFF}}{L}$	Mach 2	Mach 0.8	Mach 0.55
Measured	0.54	0.84	0.76
Calculated	0.58	0.89	0.84

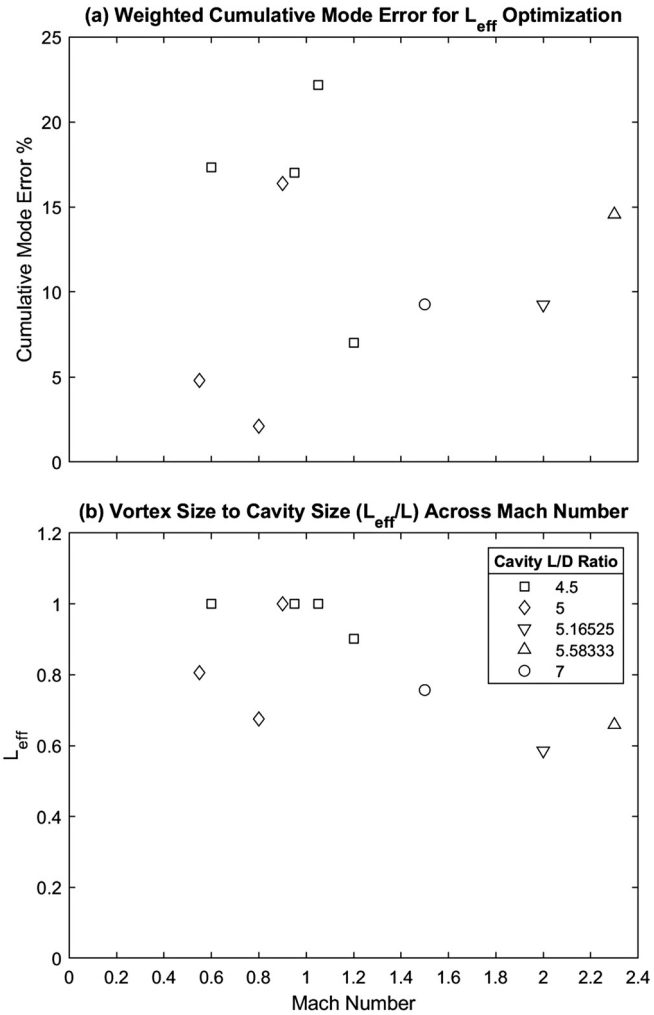

FIG. 3. Vortex length ratio optimization results across Mach number for the current method [Eq. (20)]. Panel (a) shows the weighted cumulative error of the first 5 modes for each experimental case. Panel (b) shows the calculated values of the effective length to depth (L/D) ratio and the variation in experimental L/D values for each case. The effective L/D ratios calculated from experimental results did not establish an adequate trend.

modified Rossiter and Casalino equations are so similar that they are both represented by the same points on the error graph. The results shown in Fig. 4 are in comparison to the work of Kaufman *et al.*[18] and Rossiter.[9] The Rossiter result is graphed in the Mach number range the method was initially developed for. The fractional vortex speed results derived using the modified Rossiter equation are in good agreement with Kaufman *et al.*[18] The results derived with Casalino agree better with the value 0.57 that Rossiter[9] originally derived. This is especially true for higher Mach number results. It is possible previous attempts to classify the fractional vortex speed were influenced by not including the recirculation velocity present inside the cavity, leading to a higher fractional vortex speed calculated to compensate. The trends shown here can be implemented into the Rossiter or Casalino equations to further improve accuracy.

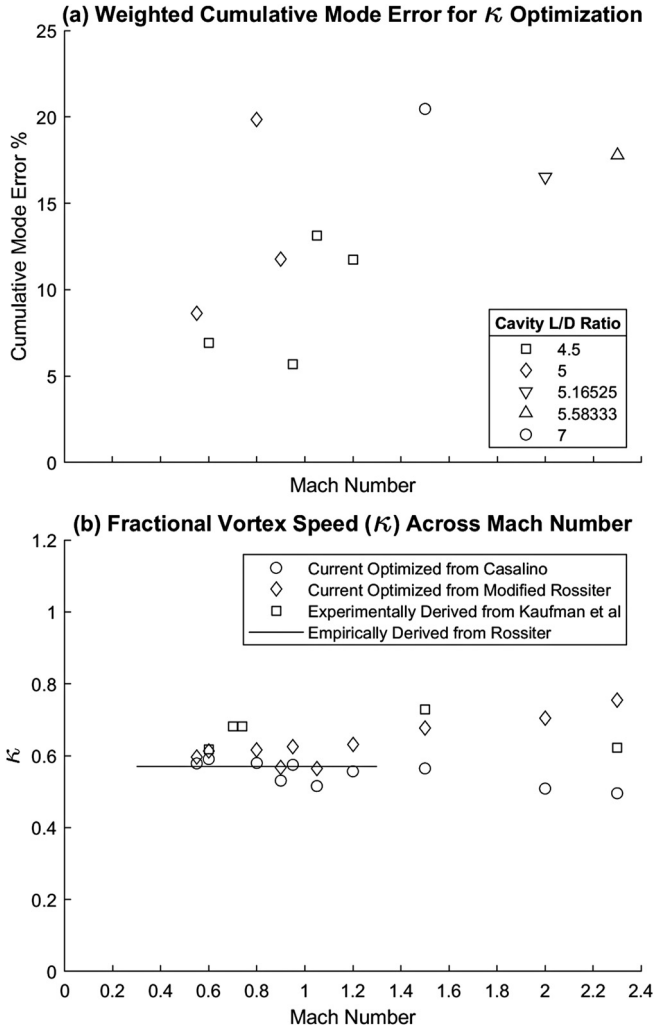

FIG. 4. Fractional vortex speed optimization results across Mach number for Rossiter and Casalino methods [Eqs. (5), (8), and (24)]. Panel (a) shows the weighted cumulative error of the first 5 modes for each experimental case with the corresponding cavity L/D ratio. Fractional vortex speed generally has lower cumulative error than the effective cavity length work in Fig. 3. Panel (b) shows the calculated values of fractional vortex speed compared to Rossiter's original results (Ref. 9) and the work of Kaufman *et al.* (Ref. 18).

IV. CONCLUSION

We reviewed existing methods for frequency prediction in cavity flows. We proposed modifications to available methods to more accurately predict the Rossiter modes present during cavity shear mode. During the shear mode, a stable vortex persists inside the cavity. At higher Mach numbers in particular, the stable vortex present inside the cavity fills only a section of the length. We derived an effective length parameter that showed good agreement with measured values from experimental work, but we were not able to fully validate the method. We synthesized the results of DeChant and Casalino into a modified method that behaves well across Mach number. The optimization algorithm we developed works favorably for the fractional vortex speed despite low data accuracy because Rossiter derived equations are less sensitive to numerical errors. This range of reported values allows one to tailor the fractional vortex speed to further improve the accuracy of any Rossiter derived method.

In future work, the effective cavity length trend could be further characterized with computational results. We predict this will also involve breaking effective length into three different flow regimes: subsonic, transonic, and supersonic. The improved fractional vortex speed can also be further improved through synthesis with computational results.

ACKNOWLEDGMENTS

The authors would like to acknowledge the Dynamics acoustics aeroelasticity Theory Experiments Computations Controls (DynaaTECC) Research Lab members for providing insightful comments during this research.

[1]D. A. Norton, "Investigation of B47 bomb bay buffet," Boeing Airplane Co., Technical Report No. D12675, Boeing Airplane Co., Seattle, WA, 1952.
[2]M. Gharib and A. Roshko, "The effect of flow oscillations on cavity drag," J. Fluid Mech. **177**, 501–530 (1987).
[3]T. M. Faure, C. L. Douay, J. Basley, H. Thach, L. R. Pastur, and F. Lusseyran, "Cavity flow stability analysis with space phase-averaged velocity fields," in *4th International Symposium Bifurcation and Instabilities in Fluid Dynamics*, Barcelona, Spain (July 1, 2011).
[4]H. H. Heller, D. G. Holmes, and E. E. Covert, "Flow-induced pressure oscillations in shallow cavities," J. Sound Vib. **18**(4), 545–546 (1971).
[5]Y. Zhang, L. Cattafesta, and L. Ukeiley, "A spectral analysis modal method applied to cavity flow oscillations," in *11th International Symposium on Turbulence and Shear Flow Phenomena (TSFP11)*, Southampton, UK (July 30 to August 2, 2019).
[6]S. Singh and L. Ukeiley, "Proper orthogonal decomposition of high-speed particle image velocimetry in an open cavity," AIAA J. **58**(7), 2975–2990 (2020).
[7]Y. Sun, A. Nair, K. Taira, L. N. Cattafesta, G. A. Brès, and L. S. Ukeily, "Numerical simulations of subsonic and transonic open-cavity flows," in *7th AIAA Theoretical Fluid Mechanics Conference*, Atlanta, GA (June 2014) (American Institute of Aeronautics and Astronautics, Reston, VA, 2014).
[8]M. Murayama, Y. Yokokawa, K. Yamamoto, and T. Hirai, "Computational study of low-noise fairings around tire-axle region of a two-wheel main landing gear," Comput. Fluids **85**, 114–124 (2013).
[9]J. E. Rossiter, "Wind tunnel experiments of the flow over rectangular cavities at subsonic and transonic speeds," R. & M. Report No. 3438, Aeronautical Research Council, London, 1964.
[10]L. DeChant, "A cavity depth sensitized Rossiter mode formula," Appl. Math. Comput. **347**, 143–148 (2019).
[11]D. Casalino, I. Gonzalez-Martino, and S. Mancini, "On the Rossiter-Heller frequency of resonant cavities," Aerosp. Sci. Technol. **131**(Part B), 108013 (2022).

[12]P. J. W. Block, "Noise response of cavities of varying dimensions at subsonic speeds," Report No. NASA TN D8351, NASA Langley Research Center, National Aeronautics and Space Administration, Langley, VA, 1976.
[13]J. L. Wagner, S. J. Beresh, K. M. Casper, B. O. Pruett, R. W. Spillers, and J. F. Henfling, "Experimental investigation of aspect-ratio effects in transonic and subsonic rectangular cavity flow," Report No. SAND2013-10639C, Sandia National Lab (SNL-NM), Albuquerque, NM, 2013.
[14]N. Zhuang, F. S. Alvi, M. B. Alkislar, and C. Shih, "Supersonic cavity flows and their control," AIAA J. **44**(9), 2118–2128 (2006).
[15]K. M. Casper, J. L. Wagner, S. J. Beresh, J. F. Henfling, R. W. Spillers, and B. O. M. Pruett, "Complex geometry effects on cavity resonance," AIAA J. **54**(1), 320–330 (2016).
[16]J. D. Anderson, *Modern Compressible Flow*, 3rd ed. (McGraw-Hill, New York, 2002).
[17]P. G. Drazin and W. H. Reid, *Hydrodynamic Stability*, 2nd ed. (Cambridge University Press, Cambridge, 2004), pp. 14–22.
[18]L. G. Kaufman, A. Maciulaitis, and R. L. Clark, "Mach 0.6 to 3.0 flows over rectangular cavities," Report No. AFWAL-TR-82-3112, Flight Dynamics Laboratory, Air Force Wright Aeronautical Laboratories, Air Force Systems Command, United States Air Force, Wright-Patterson AFB, OH, 1983.
[19]R. C. Bauer and R. E. Dix, "Engineering model of unsteady flow in a cavity," Accession No. ADA243636, Arnold Engineering Development Center, Air Force Systems Command, United States Air Force, Arnold AFB, TN, 1991.